

Design and Applications of Yb/Ga₂Se₃/C Schottky Barriers

Hazem K. Khanfar, *Member, IEEE*, Atef F. Qasrawi, Yasmeeen A. Zakarneh, and N. M. Gasanly

Abstract—In this paper, the Ga₂Se₃ crystals are used to design a Yb/Ga₂Se₃/C Schottky barrier. The device structure is investigated by the X-ray diffraction technique, which reveals a monoclinic-face-centered cubic interfacing type of structure. The barrier is studied by means of current (*I*)–voltage (*V*) characteristics in the dark and under light through photoexcitation from tungsten lamp and from the He–Ne laser. In addition, the impedance spectroscopy of these devices is studied in the frequency range of 10–1400 MHz. The photoexcited *I* – *V* curve analysis allowed investigating the biasing voltage, illumination power, and energy effects on the diode physical parameters, which are presented by the rectification ratio, the Schottky barrier height, the ideality factor, the series resistance, the photosensitivity, the responsivity, and the external quantum efficiency (EQE). While a maximum photosensitivity of 42 was observed for laser excitation with a wavelength of 632 nm at a reverse bias of 4.4 V, the EQE reached value of 1652% at 19.0 V. On the other hand, the ac current conduction analysis of the electrical conductivity, which was determined from the impedance spectral analysis, indicated that the ac signal processing through the Yb/Ga₂Se₃/C samples is due to the correlated hopping conduction through localized states of Fermi density of $3.98 \times 10^{19} \text{ eV}^{-1} \text{ cm}^{-3}$. The high-and biasing-dependent EQE% nominates the Yb/Ga₂Se₃/C as a tunable optoelectronic device.

Index Terms—Optical materials, Ga₂Se₃ crystals, optoelectronic, impedance.

I. INTRODUCTION

LAYERED crystals Ga_xSe_y have attracted remarkable interest of researchers and industry sectors owing to their applications as smart materials for sensing. Nonlinear gallium selenide (GaSe) crystals are reported to be able to generate broadband emission from the near infrared (IR) (0.8 μm) through the mid- and far-IR (terahertz (THz)) ranges and extends to the millimeter wave (5.64 mm) range [1]. In another work, through trails to generate terahertz pulses from GaSe

Manuscript received March 27, 2017; accepted May 6, 2017. Date of publication May 9, 2017; date of current version June 23, 2017. This work was supported by the Scientific Research Council, Arab American University in Jenin during 2015–2016. The associate editor coordinating the review of this paper and approving it for publication was Prof. Alexander Fish. (Corresponding author: Atef F. Qasrawi.)

H. K. Khanfar is with the Department of Telecommunication Engineering, Arab American University of Jenin, Jenin 240, Palestine (e-mail: Hazem.Khanfar@aaup.edu).

A. F. Qasrawi is with the Departments of Physics, Arab American University of Jenin, Jenin 240, Palestine, and also with the Group of Physics, Faculty of Engineering, Atılım University, 06836 Ankara, Turkey (e-mail: atef.qasrawi@atilim.edu).

Y. A. Zakarneh is with the Department of Physics, Arab American University of Jenin, Jenin 240, Palestine.

N. M. Gasanly is with the Department of Physics, Middle East Technical University, Ankara 06800, Turkey (e-mail: nizami@metu.edu.tr).

Digital Object Identifier 10.1109/JSEN.2017.2702710

layers [2] it was observed that by controlling the concentration of sulfur in the GaSe:S crystals, the efficiency of generation of terahertz radiation which was measured by the optical rectification of femtosecond laser pulses technique, is improvable. In addition, studies on the effects of different gas molecules on the photoelectric response of few-layer GaSe phototransistors before and after introducing defects have shown that, when thermally annealed, the phototransistors of GaSe can exhibit a large photo-responsivity (18.75 A/W) with high external quantum efficiency (EQE) (similar to 91.53%), high photocurrent on-off ratio, fast photo-response, and good stability in an O^{−2} rich environment when illuminated by 254 nm ultraviolet light [3].

Previous studies on the band structure of Ga₂Se₃ have revealed that the band-gaps of monoclinic structured Ga₂Se₃ is 2.53 eV and that of the orthorhombic is 2.2 eV [4]. It was also shown that the band-gap cutoff wavelength of the Ga₂Se₃ can be lowered to the thermal infrared region through the antireflective coating which allows chemical durability of the GeSe₂-Ga₂Se₃ glassy matrix [5], [6].

The Ga₂Se₃ also occurs under normal conditions in two modifications. The zincblende type α-Ga₂Se₃ which exhibit disordered vacancies and lattice parameter of 5.418°Å and energy band gap of 1.92-1.79 eV and the one with the ordered vacancies β-Ga₂Se₃ [7]. The latter's energy band gap and lattice parameters are 2.0 eV and *a* = 23.235 and *c* = 10.828°Å.

These optoelectronic properties of the Ga₂Se₃ make it attractive for the fabrication of light sensitive sensors that can perform in wide range of light spectrum. As announced, on the website, by the IEEE sensors council in their field of interest in the branch of optoelectronic/photonic sensors all photovoltaic diodes, photodiodes, phototransistors and position-sensitive photodetectors, as well as in the branch of the microwave/millimeter wave sensors are all regarded as sensor class that are worth of consideration by the IEEE sensors journal and other related journals. Thus, based on these information, here in this work, we attempt to establish applications for the Ga₂Se₃ crystal in the visible as well as in the IR region of light spectrum. Particularly, the Ga₂Se₃ crystals are employed to construct a Yb/Ga₂Se₃/C Schottky device. The device will be characterized by means of current-voltage characteristics and impedance spectroscopy. The visible-IR irradiation to the crystal will be supplied from tungsten lamp. In addition, for particular applications as a photosensor to He-Ne lasers, the crystal is irradiated with a 632 nm laser source. The resulting responsivity, photosensitivity and exter-

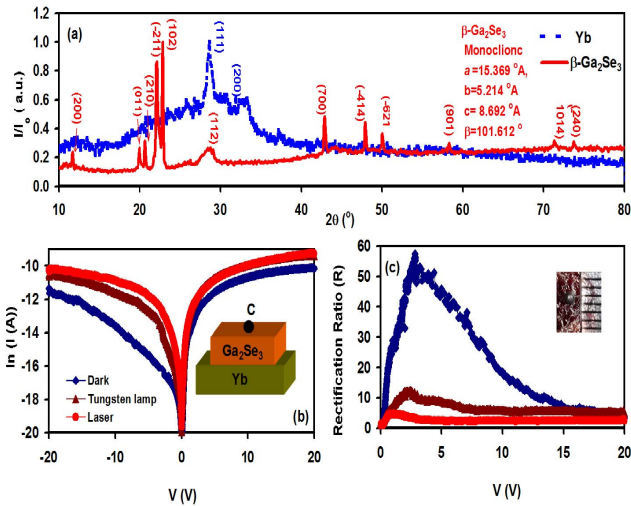


Fig. 1. (a) The X-ray diffraction patterns for Yb and Ga_2Se_3 crystals. (b) The current-voltage characteristics in the dark and under photoexcitation. (c) The rectification ratio as a function of applied voltage for the Yb/ Ga_2Se_3 /C Schottky diodes.

nal quantum efficiency will be discussed. In addition, some information which relates to AC signal processing will also be provided.

II. EXPERIMENTAL DETAILS

Ga_2Se_3 crystal lumps of 99.99% (Alfa Aesar CAS No: 12024-24-7) were used as substrates for the deposition of ytterbium thin films under a vacuum pressure of 10^{-5} mbar. The X-ray diffraction patterns for the substrate and the crystal were recorded with the help of Rigaku miniflex 600 X-ray diffraction unit. The top part of the crystal was contacted with carbon paste (PELCO # 1602). This carbon paste forms a thin, conductive and flexible layer (sheet) with excellent adhesion. The carbon circular point of area $7.85 \times 10^{-3} (\text{cm}^2)$ was left to dry for 24 hours. The geometrical and actual top view of the device is displayed in the insets of Fig. 1. The current-voltage characteristics of the device were recorded using a Keithley current-voltage characterization system. The light illumination was supplied from an incandescent tungsten lamp and by using a 1 mW He-Ne laser source of single radiation of the 632 nm laser line. The light power was recorded with the help of a radiometer. The spectrum of the tungsten lamp which ranges 400 to 2000 nm exhibits maximum radiation near 900 nm. The radiation power of this lamp is altered by controlling the distance between the sample and the source. On the other hand, the impedance spectra were recorded using Agilent 4291B 0.01-1.80 GHz impedance analyzer. The connections to the fixtures (the 16193A small side electrode, 16453A dielectric material test fixture, and Hp16192 A/70 side electrode test fixture) were made by AP-7 connector attached to the analyzer.

III. RESULTS AND DISCUSSION

A. Structural Analysis

The X-ray diffraction patterns for the $1.0 \mu\text{m}$ thick Yb film and for the $100 \mu\text{m}$ thick Ga_2Se_3 crystals are shown

in Fig. 1 (a). The X-ray diffraction patterns for both materials are analyzed using “TREOR 92” software package. While the Yb film is observed to exhibit a cubic crystal structure of lattice parameter of $a = 5.487 \text{ \AA}$ (PDF card no:00-002-1367), the Ga_2Se_3 is observed to be of β -type polymorphic modification that exhibits a monoclinic crystal structure of lattice parameters of $a = 15.369$, $b = 5.214$, $c = 8.692 \text{ \AA}$ and $\beta = 101.612^\circ$. The different values of the lattice parameters from that of literature [4], [7] probably arise from the ordering mechanism of the vacancies in the structure. The lattice mismatches ($\Delta\% = 100 \times a_{\text{Ga}_2\text{Se}_3} - a_{\text{Ga}_2\text{Se}_3}$) between the crystal and the Yb film along the a -axis, b -axis, and c -axis are 64.3%, 5.2% and 36.9%, respectively. The values along the a and the c -axis are large compared to that of b -axis and usually causes charge accumulation at the Yb/ Ga_2Se_3 interface. Such property could be beneficial in lowering the leakage current of Schottky barriers [8]–[10].

B. Dark and Photoelectrical Characterization

The geometrical design of the Yb/ Ga_2Se_3 /C Schottky device is shown as an inset in Fig. 1 (b). The figure also displays the current-voltage characteristic curve for the Schottky device in the dark. As it is observable from Fig. 1 (b), the value of the forward biased current under illumination is larger than that of dark. The same behavior is also observed for the reverse biased currents. In the dark at a particular voltage value of 10 V, for example, while the forward biased current exhibit value of 2.25×10^{-5} A the reverse biased current exhibit value of 1.23×10^{-6} A. When exposed to laser light of 632 nm wavelength, the forward current raises to 4.68×10^5 A and the reverse current raises to 1.86×10^5 A. While the forward biased current duplicates, the reverse increases 15 times. The dark forward (I_F) to the reverse (I_R) current rectification ratio ($R = I_F/I_R$) as a function of biasing voltage is shown in Fig. 1 (c). As the latter figure reads, the dark current rectification ratio increases with increasing biasing voltage. It reaches a value of ~ 58 at a critical biasing voltage (V_C) of 2.82 V. For higher applied voltage values, the rectification ratio sharply decreases with increasing voltage reaching a value of 4.40 at 20 V. On the other hand, subjecting the Schottky barrier device to light excitation from a tungsten lamp of light power of $379 \mu\text{W}$ and from a He-Ne laser light (632 nm) of power of 1.0 mW decreased the values of maximum R from 58 in the dark to 12 and to 4.53, respectively. Consistently, the biasing critical voltage where the maximum R value was observed in the dark (2.82 V) lowers to 2.15 and 0.80 V, respectively. This behavior is ascribed to the intensity and energy of incident photons. The more intensive and energetic the incident light, the more photons, the more generated electron hole pairs. As the electron hole pair are separated by the applied electric field, the current increases in a particular direction leading to a decrease in the rectification voltage as a result of resistance lowering compared to dark value as will be seen in the forthcoming discussion. The increase in the reverse current with increasing illumination intensity, which is expectedly results from the generated electron-hole pairs, assures the photovoltaic characteristics of the Yb/ Ga_2Se_3 /C device.

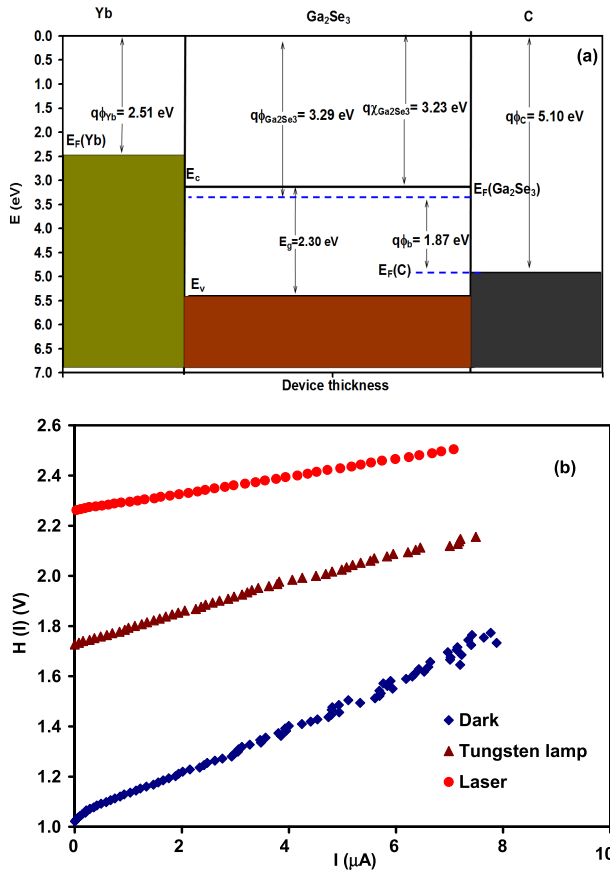


Fig. 2. (a) The theoretical energy band diagram. (b) The Cheung function for the Yb/Ga₂Se₃/C Schottky diodes.

The theoretical energy band diagram of the Yb/Ga₂Se₃/C Schottky device which is shown in Fig. 2 (a) is designed based on literature data [11]–[13] which indicated that the Ga₂Se₃ crystals exhibits an electron affinity ($q\chi_{Ga_2Se_3}$) of 3.23 eV [12]. The Fermi level is accepted to be 0.055 eV below the bottom of the conduction band, (the donor energy level of the Ga₂Se₃ crystals is experimentally determined through temperature-dependent resistivity measurements to be 0.11 eV below the bottom of the conduction band). Thus, the work function of the crystal is 3.29 eV. The metallic sides of the device exhibit work functions of $q\phi_{Yb} = 2.51$ [9] and $q\phi_C = 5.1$ eV [13] for Yb and C, respectively. On the other hand, the energy barrier height ($q\phi_b = q\phi_C - q\chi_{Ga_2Se_3}$) and built in voltage for this device ($qV_{bi} = q\phi_C - q\phi_{Ga_2Se_3}$) is determined as 1.87 and 1.81 eV, respectively.

In the light of the above mentioned numerical values, the decrease in the rectification ratio of the dark current for applied voltages greater than 2.82 eV, may be probably ascribed to the decrease in the space-charge depletion width at the Carbon- Ga₂Se₃ Schottky contact interface, and/or possibly due to the work function difference of the two different electrode materials as well as the different mobility of electron and holes within the bicontinuous interpenetrating network of two components [11]. The assignment of the decrease in the R values at V_C to the difference (2.81 eV) in the metals work function appears to be more reasonable as it suggests closer voltage values to $V_C = 2.51$ eV of the dark current.

TABLE I
PHYSICAL PARAMETERS FOR Yb/Ga₂Se₃/C SCHOTTKY DIODES

$F(\mu W)$	n	$q\phi_b$ (eV)	R (kΩ)
Dark	1.51	1.58	419
61	2.20	1.79	251
75	2.53	2.03	236
379	2.22	2.15	162
Laser	3.04	2.60	194

In order to understand the reason(s) for the decrease in the values of R and V_C under photoexcitation, the $I - V$ characteristics of the device is analyzed assuming the domination of the Richardson-Schottky current conduction by thermionic emission of charged particles over an energy barrier of height of $q\phi_b$ [14], [15]. The thermionic emission theory assumes that only energetic carriers which have an energy equal to or larger than the conduction band energy at the metal-semiconductor interface, contribute to the current flow.

The device's current is defined by the relation,

$$I = AA * T^2 \exp\left(\frac{-q\phi_b}{kT}\right) \left(\exp\left(\frac{q(V - IR_s)}{nkT}\right) - 1\right). \quad (1)$$

In (1), A is the diode area, $A^* = 23.06$ is Richardson constant [12], R_s is the series resistance, n is the ideality factor and T is the temperature. Equation (1) was employed by I. Orak et al. [14] to determine the effect of annealing temperature on the series resistance of the diode that directly influence barrier height and ideality factor. Similarly, and M. A. Mayimele et al. [15] use this formalism with the associated Cheung's function to derive the series resistance effect on the barrier height and ideality factor as function of temperature in the range of 80-320 K. By calculating the derivative $dV/d \ln(I) = IR_s + n(kT/q)$ and plotting it as a function of I , one can determine the value of the ideality factor n and R_s . Substituting the value of n into Cheung's function ($H(I)$) through the relation [15],

$$H(I) = V - n \left(\frac{kT}{q}\right) \ln\left(\frac{I}{AA * T^2}\right) = IR_s + nq\phi_b, \quad (2)$$

it is possible to calculate the value of $q\phi_b$. Here, the factor IR_s represents the voltage drop across the series resistance of the Schottky diode. The Cheung's function analytical method assumes that the ideality factor could be larger than one and that the barrier height is independent of biasing voltage at particular temperature. The plot of $H(I)$ versus I which is representatively displayed in Fig. 2 (b) reveals the ideality factor, the series resistance and the barrier heights. These physical parameters are shown in Table I. Similar results which concern series resistance lowering associated with increased barrier height and decreased ideality factor as function of increasing temperature was observed for Co/GaP diodes [14] and for the Pd/ZnO Schottky barriers [15]. The behavior was assigned to increase in the free carrier density that occurs due to the diffusion of metals from the surface to the bulk of semiconductor [14].

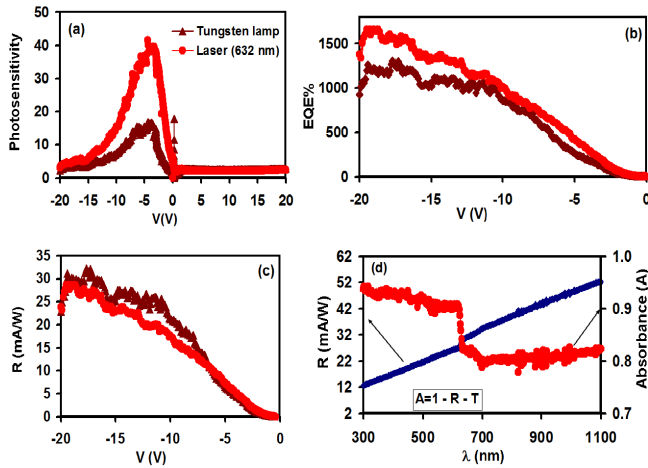


Fig. 3. The voltage biasing dependences of: (a) photosensitivity, (b) external quantum efficiency, and (c) the responsivity of the Yb/Ga₂Se₃/C Schottky diodes for tungsten lamp and He-Ne laser light. (d) The spectral response and absorbance of the device.

Even though, the series resistance effect on the ideality factor and barrier height is reduced through the use of (1) and (2), the value of n which is evaluated from the dark I - V data is still greater than unity indicating that the photodiodes exhibit a non-linear behavior. This deviation from unity can be assigned to the particular distribution of the interface states, the presence of inhomogeneities of the barrier height, and generation-recombination currents within the space-charge region [16], [17].

In general, under photoexcitation of tungsten light, the values of the energy barrier height and of the ideality factor are increasing with increasing illumination intensity. Oppositely, the value of the series resistance decreases with increasing illumination intensity. On the other hand, the light of He-Ne laser caused a re-increase in the series resistance in spite of the power being larger. The maximum energy of photons supplied from incandescent lamp is 1.38 eV and that of the laser is 1.97 eV. Both values are less than the direct allowed transition energy band gap (2.30 eV). That type of behavior during the working process of Schottky diode under light illumination can be understood by recalling that the light generates hole-electron pairs, while the holes drift with the applied electric field to the negative contact, the electrons drift to the positive side. At particular photon energy where the kinetic energy of photons is constant, increasing the photons intensity increases the number of the generated electron-hole pairs. The increase in the generated pairs increases the recombination rates at the carbon and ytterbium sides. In addition, the capturing of photogenerated carriers by the localized energy trap regions causes accumulation of charge carriers in the vicinity of the Schottky barrier, especially at the edges of the metal contact where the electric field is very strong [16], [17]. The data presented in Fig. 3 (a), represent the effect of biasing voltage on the photosensitivity of the device. As it is easily observed from the figure, the photosensitivity (I_L/I_d) of the Schottky device under the reverse bias conditions is much larger, compared to the forward biased, indicating

that the photocurrent is dominated the avalanche process. This process occurs when carriers in the transition region are accelerated by the electric field to energies sufficient to create mobile or free electron-hole pairs via collisions with bound electron. In addition, photosensitivity, which exhibits the value of 42 under monochromatic laser light, is nearly three times larger than of tungsten light at 4.4 volts. The voltage region of 3.5-6.2 V exhibits, approximately, constant values of photosensitivity. For applied reverse biasing voltages larger than 6.2 V, the photosensitivity sharply falls reaching a value of ~ 2.2 at 20.0 V. The latter behavior could have raised from the generation of avalanche current under the influence of strong electric field. The avalanche process occurs when carriers in the transition region are accelerated by the electric field to energies sufficient to create mobile or free electron-hole pairs via collisions with bound electrons [18].

The external quantum efficiency (EQE) for the Yb/Ga₂Se₃/C Schottky photodiodes which is shown in Fig. 3(b) is calculated from the relation,

$$EQE = (I_L - I_d)hv / (I_{in}e) \quad (3)$$

with hv being the incident photon energy and I_{in} is the incident light intensity [19]. The EQE equation is limited by the optical transmittance at particular wavelength in which current can be evaluated up to maximum absorbed wavelength [20]. The figure displays comparative values of EQE for both excitation types. The wavelength of the incident light from tungsten was taken as 900 nm which is the highest point of the tungsten radiation spectra in the range of 400-2000 nm. For both types of excitation, the external quantum efficiency of the device being larger than 1650 (at 19.0 V) is of acceptable values compared to values reported in literature [19]. It is also possible to improve the device efficiency through resistance permanent lowering via annealing process. The metals on the surface of sample diffuse into semiconductor with increasing annealing temperature and so carrier density is expected to increase, and thus, resistance decreases [14].

Studies on Ga₂O₃ in thin film and crystal forms displayed EQE values of 18, 1600, 17, 4350, 5×10^5 , 34 and $1.8 \times 10^5\%$ for Ga₂O₃ metal-semiconductor-metal thin films, nanosheets, nanowire, Schottky photodetector, single crystal, Ga₂O₃/SiC heterojunction and Ga₂O₃/ p -Si devices, respectively [19]. Since the avalanche effect is dominant during the reverse biasing process of the Yb/Ga₂Se₃/C photodiodes, the external quantum efficiency of these photodetectors is probably governed by the avalanche multiplication mechanism. Photo-generated carriers contribute to the avalanche multiplication through impact ionization [19]. Another reason which could contribute to the high EQE is the photoconductive gain in which the responsivity saturates at elevated bias. The photodiode responsivity (R) dependence on the biasing voltage which is shown in Fig. 3 (c) suggests that both mechanisms contribute to the high EQE of the device. Namely, for low applied voltages (less than ~ 2.5 V), the R - V dependence is exponentially varying indicating the domination of avalanche multiplication mechanism. For higher applied voltages, the R - V dependence follows a slower trend indicating the photoconductive gain effects [19].

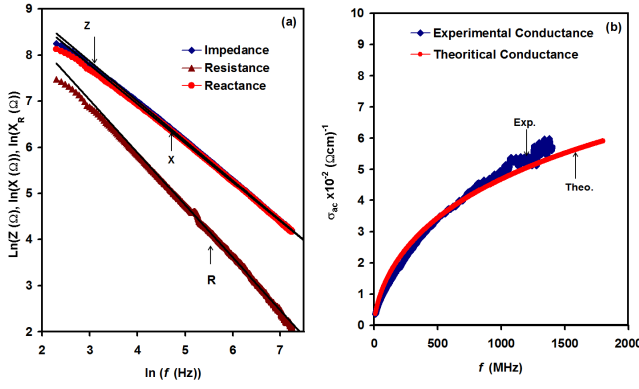


Fig. 4. (a) The impedance, resistance and reactance spectra. (b) The AC conductivity spectra for the Yb/Ga₂Se₃/C Schottky diodes being recorded in the frequency range of 10-1400 MHz.

As complementary data, the spectral response of the device is determined and displayed in Fig. 3 (d). The spectral response is calculated from the measured reflectance (\bar{R}), transmittance (T) and absorbance ($A = 1 - \bar{R} - T$) spectral data in the incident light wavelength (λ) range of 300-1100 nm using the relation [21],

$$R = (1 - \bar{R}) \times EQE / (A \times 1243 / \lambda(\text{nm})). \quad (4)$$

The spectral response continuously increases with increasing incident light wavelength. It exhibits a jump at 622 nm. This value is very close to the absorption edge which also appears on in Fig. 3 (d). As also seen from the figure, the responsivity did not reach the cutoff point near the band gap ($E_g = 1.85$ eV). This behavior which can be regarded as an advantage as it allows responsivity of wider range of spectrum could be assigned to the interband transitions in the Ga₂Se₃ crystals [21].

C. Impedance Spectroscopy

As another type of application, the Yb/Ga₂Se₃/C Schottky device was tested with an impedance analyzer that allow AC signal propagation in the frequency range of 10 -1800 MHz. The input signal amplitude was ~ 0.10 V. The analyzer reads the impedance (Z), the resistance (X_R) and the reactance (X) as a function of AC signal frequency (f). Accurate data recording was possible up to 1400 MHz. The Z , X_R and X spectral data which is displayed in Fig. 4 (a) suggest the, Z , X , $X_R \propto f^q$, relationship. The q value which is obtained from the linear slopes of the $\ln(Z) - \ln(f)$, $\ln(X) - \ln(f)$ and $\ln(X_R) - \ln(f)$ dependencies are found to be 0.86, 0.85 and 1.14, respectively.

It is also readable from the figure that the impedance value is approximately the same as that of the (capacitive-inductive) reactance. The resistive part of reactance is of less effect on the total impedance. Such property indicates that the device under test behaves mostly as a capacitor. To give significance for the numerical values of q under, approximately, no biasing conditions we have calculated the AC conductivity spectra from the relationship between the admittance ($1/Z$) and the

conductance,

$$G = X_R / (X_R^2 + X^2). \quad (5)$$

The AC conductivity ($G = \sigma_{ac} \cdot l / A$; $l = 0.10$ cm) spectra which are shown in Fig. 4 (b) exhibit a different type of variation from that of the impedance. Again, it can be presented by the relation, $\sigma_{ac} \propto f^q$. The frequency exponent (q) for the Yb/Ga₂Se₃/C device is 0.60. The increase of σ_{ac} with frequency in the frequency range of 100-1400 MHz under no biasing conditions is ascribed to the domination of the correlated barrier hopping mechanism (CBH) [22], [23], where,

$$q = 1 - 6kT / (W_M + kT \ln(\omega \tau_o)) \quad (6)$$

with W_M and τ_o are being the maximum barrier height at infinite intersite separation (binding energy of the carrier in its localized site) and the relaxation time, respectively. The CBH model assumes that the electrons hop between pairs of localized states at the Fermi level and relates the conductivity to the density of states ($N(E_F)$) at the Fermi level through the relation [22], [23],

$$\sigma_{ac} = (\pi/3) e^2 k T \omega \zeta^5 (N(E_F))^2 (\ln(v_{ph}/\omega))^4. \quad (7)$$

Here, $\zeta = 10^9$ Å is the typical localization length and $v_{ph} = 10^{12}$ Hz is the phonon frequency. The fitting of the experimental data of conductivity in accordance with (6) that reveals the exact frequency exponent parameter ($q = 0.60$) which is shown in Fig. 4 (b) as red colored allowed determining the value of $N(E_F)$ as $3.98 \times 10^{19} \text{ eV}^{-1} \text{ cm}^{-3}$. The corresponding maximum barrier height at infinite intersite separation W_M and τ_o are found to be 0.53 eV and 1.9 ns, respectively. The value of W_M is close to that reported as 0.485 eV for Ga₂S₃-Ga₂Se₃ solid solution [22]. Other parameters are also consistent with literature data [23].

IV. CONCLUSION

In this article we have explored some particular applications of the monoclinic Ga₂Se₃ crystals through the design and characterization of the Yb/ Ga₂Se₃/C Schottky barriers. The designed band diagram of the device was compared to the experimentally determined physical parameters of the device. The photoexcitation by means of tungsten lamp and He-Ne laser revealed relatively high external quantum efficiency (EQE) associated with biasing dependent responsivity. The evaluated photoconductive parameters which are presented by the photosensitivity, responsivity, and EQE are promising as they indicate the usability of the device as a photosensor with high responsivity at 632 nm (the red colored laser) and as a photovoltaic device. In addition, the AC signal analysis of the device in the frequency range of 1-1400 MHz, nominates it for applications at microwave levels.

ACKNOWLEDGMENT

The authors acknowledge with thanks the scientific research committee at the Arab American University, Jenin, presented by the Dean of Scientific Research Prof. Dr. M. Awad for financial supporting of this research.

REFERENCES

- [1] J. Guo *et al.*, "Doped GaSe crystals for laser frequency conversion," *Light Sci. Appl.*, vol. 4, p. e362, Apr. 2015.
- [2] S. A. Bereznaya *et al.*, "Transmission spectra and generation of terahertz pulses in SiO₂-GaSe, TiO₂-GaSe, Ga₂O₃-GaSe, and GaSe:S structures," *Russian Phys. J.*, vol. 58, no. 8, pp. 1181–1185, 2015.
- [3] S. Yang *et al.*, "Highly efficient gas molecule-tunable few-layer GaSe phototransistors," *J. Mater. Chem. C*, vol. 4, no. 2, pp. 248–253, 2016.
- [4] G.-Y. Huang, N. M. Abdul-Jabbar, and B. D. Wirth, "Theoretical study of and : Band-gap engineering," *Acta Mater.*, vol. 71, pp. 349–369, Jun. 2014.
- [5] A. Bréhault *et al.*, "Multispectral glasses transparent from the visible up to the thermal infrared in GeSe₂-Ga₂Se₃-CsI system," *Mater. Techn.*, vol. 103, no. 4, pp. 403-1–403-7, 2015.
- [6] M. A. T. Marple *et al.*, "Structure and physical properties of glasses in the system Ag₂Se-Ga₂Se₃-GeSe₂," *J. Non-Crystalline Solids*, vol. 437, pp. 34–42, Jan. 2016.
- [7] O. Madelung, *Semiconductors: Data Handbook*, 3rd ed. Berlin, Germany: Springer, 2012.
- [8] C. Chen, S. Chu, and A. Cho, "GaAs/Ga_{0.47}In_{0.53}As lattice-mismatched Schottky barrier gates: Influence of misfit dislocations on reverse leakage currents," *Appl. Phys. Lett.*, vol. 46, no. 12, pp. 1145–1147, 1985.
- [9] H. L. Skriver and N. M. Rosengaard, "Surface energy and work function of elemental metals," *Phys. Rev. B, Condens. Matter*, vol. 46, no. 11, pp. 7157–7168, Sep. 1992.
- [10] W. Feng *et al.*, "Performance improvement of multilayer InSe transistors with optimized metal contacts," *Phys. Chem. Chem. Phys.*, vol. 17, no. 5, pp. 3653–3658, 2015.
- [11] D. Chirvase *et al.*, "Temperature dependent characteristics of poly(3 hexylthiophene)-fullerene based heterojunction organic solar cells," *J. Appl. Phys.*, vol. 93, no. 6, pp. 3376–3383, 2003.
- [12] R. R. N. Kmail and A. F. Qasrawi, "Physical design and dynamical analysis of resonant-antiresonant Ag/MgO/GaSe/Al optoelectronic microwave devices," *J. Electron. Mater.*, vol. 44, no. 11, pp. 4191–4198, 2015.
- [13] N. de Jonge *et al.*, "Characterization of the field emission properties of individual thin carbon nanotubes," *Appl. Phys. Lett.*, vol. 85, no. 9, pp. 1607–1609, 2004.
- [14] I. Orak, K. Ejderha, and E. Sönmez, "The effect of annealing temperature on the electrical characterization of Co/n type GaP Schottky diode," *Mater. Res. Bull.*, vol. 61, pp. 463–468, Jan. 2015.
- [15] M. A. Mayimele *et al.*, "Analysis of temperature-dependant current-voltage characteristics and extraction of series resistance in Pd/ZnO Schottky barrier diodes," *Phys. B, Condens. Matter*, vol. 480, pp. 58–62, Jan. 2016.
- [16] A. S. Dahlan *et al.*, "Photodiode and photocapacitor properties of Au/CdTe/p-Si/Al device," *J. Alloys Compound*, vol. 646, pp. 1151–1156, Oct. 2015.
- [17] H. K. Khanfar and A. F. Qasrawi, "Performance of the Au/MgO/Ni photovoltaic devices," *Mater. Sci. Semicond. Process.*, vol. 29, pp. 183–187, Jan. 2015.
- [18] S. Lei *et al.*, "An atomically layered InSe avalanche photodetector," *Nano Lett.*, vol. 15, no. 5, pp. 3048–3055, 2015.
- [19] X. C. Guo *et al.*, " β -Ga₂O₃/p-Si heterojunction solar-blind ultraviolet photodetector with enhanced photoelectric responsivity," *J. Alloys Compounds*, vol. 660, pp. 136–140, Mar. 2016.
- [20] J. D. Servaites, M. A. Ratner, and T. J. Marks, "Practical efficiency limits in organic photovoltaic cells: Functional dependence of fill factor and external quantum efficiency," *Appl. Phys. Lett.*, vol. 95, no. 16, p. 163302, 2009.
- [21] H. Zimmermann, *Integrated Silicon Optoelectronics*. Berlin, Germany: Springer, 2009, pp. 1–9.
- [22] A. E. Bekheet, "AC conductivity and dielectric properties of Ga₂S₃-Ga₂S₃ films," *Phys. Rev. B, Condens. Matter*, vol. 403, nos. 23–24, pp. 4342–4346, 2008.
- [23] A. A. A. Darwish, M. M. El-Nahass, and A. E. Bekheet, "AC electrical conductivity and dielectric studies on evaporated nanostructured InSe thin films," *J. Alloys Compounds*, vol. 586, pp. 142–147, Feb. 2014.



Hazem K. Khanfar (M'11) received the M.S. degree in telecommunication and electronics from the Jordan University of Science and Technology, Irbid, Jordan, in 2004, and the Ph.D. degree in electrical engineering from the University of New Orleans, New Orleans, LA, USA, in 2009. He is currently an Associate Professor with the Faculty of Engineering and IT, Arab American University of Jenin, Jenin, Palestine. His current research interests include thin-film solid states, design of tunneling diodes, and signal processing.



Atef F. Qasrawi was born in Palestine in 1968. He received the B.Sc., M.S., and Ph.D. degrees in physics from Middle East Technical University, Ankara, Turkey, in 1994, 1997, and 2000, respectively. He is currently a Full Professor of Physics with the Department of Physics, Arab American University of Jenin, Jenin, Palestine, and the Physics Group, Atılım University, Ankara. His research includes experimental and computational solid-state physics and electronics. His current research focuses on the design and characterization of microwave tunneling devices, and pyrochlore ceramics. He received over 15 researcher awards, and has over 110 Thomson-ISI publications in solid-state physics and electronics. His ISI-citation record exceeded 530 according to the 2014 statistics.

Yasmeen A. Zakarneh received the B.Sc. degree in physics from Arab American University of Jenin, Palestine, in 2015. Her current research interests include electrical characterization of solid materials.



N. M. Gasanly received the M.S. degree from Baku State University, Baku, Azerbaijan, in 1963, and the Ph.D. degree from the Physico-Technical Institute, Leningrad, Russia, in 1972. He joined Baku State University in 1972. Since 1992, he has been a Visiting Professor with Middle East Technical University, Ankara, Turkey. He has co-authored over 267 scientific papers.